Cellular Immunology 344 (2019) 103946

Contents lists available at ScienceDirect

Cellular Immunology

journal homepage: www.elsevier.com/locate/ycimm

Research paper

Multi-modal image cytometry approach – From dynamic to whole organ imaging

Nazihah Husna[a,b], Nicholas R.J. Gascoigne[b], Hong Liang Tey[c,d,e], Lai Guan Ng[a,b,*], Yingrou Tan[a,c,*]

[a] Singapore Immunology Network (SIgN), A*STAR (Agency for Science, Technology and Research), Biopolis, 8A Biomedical Grove, Singapore 138648, Singapore
[b] Department of Microbiology and Immunology, Yong Loo Lin School of Medicine, National University of Singapore, 5 Science Drive 2, Singapore 117545, Singapore
[c] National Skin Centre, 1 Mandalay Road, Singapore 308205, Singapore
[d] Lee Kong Chian School of Medicine, Nanyang Technological University, 11 Mandalay Road, Singapore 308232, Singapore
[e] Yong Loo Lin School of Medicine, National University of Singapore, 10 Medical Dr, Singapore 117597, Singapore

ARTICLE INFO

Keywords:
Image cytometry
Image analysis
Intra-vital imaging
Optical clearing
Whole mount imaging

ABSTRACT

Optical imaging is a valuable tool to visualise biological processes in the context of the tissue. Each imaging modality provides the biologist with different types of information – cell dynamics and migration over time can be tracked with time-lapse imaging (e.g. intra-vital imaging); an overview of whole tissues can be acquired using optical clearing in conjunction with light sheet microscopy; finer details such as cellular morphology and fine nerve tortuosity can be imaged at higher resolution using the confocal microscope. Multi-modal imaging combined with image cytometry – a form of quantitative analysis of image datasets – provides an objective basis for comparing between sample groups. Here, we provide an overview of technical aspects to look out for in an image cytometry workflow, and discuss issues related to sample preparation, image post-processing and analysis for intra-vital and whole organ imaging.

1. Introduction

In comparison to other techniques such as flow cytometry, mass cytometry, RNA sequencing or enzyme-linked immunosorbent assays, imaging experiments can be comparatively more tedious, have a lower throughput and requires specific technical know-how and trained personnel to carry out. Why then is imaging valuable?

The key advantage of imaging is the capability to visualise cellular components in the context of the entire tissue. Tissue dissociation or lysis is typically required to release cells or genetic material from the tissue for analysis, but in this process, information such as cell–cell interactions, cellular behaviour and localization is lost. Tissue dissociation protocols can also vary between laboratories, and enzymatic digestion using trypsin or Type IV collagenase is also known to cause cleavage of some surface receptors [1]. Imaging is thus a valuable tool for visualising cellular distribution *in situ* without disrupting the architecture of the tissue, preserving the spatial information.

Imaging modalities for biological discovery are ultimately dependent on technological developments in imaging hardware and software. Antonie van Leeuwenhoek and Robert Hooke, widely regarded as the pioneers of the field of microbiology for their observations of protozoa, were able to make their discoveries by designing the most primitive form of the microscope using glass lenses [2]. Recent technological advances in the field of optical imaging have provided the biologist with a plethora of techniques such as: intra-vital two-photon microscopy to track cellular activity and changes over space and time; light sheet microscopy for whole organ imaging coupled with optical clearing to provide an overview of any changes in the tissue; and confocal microscopy to interrogate specific regions within the tissue at higher resolution. Together, these techniques can be used in combination in an imaging workflow to provide a multi-faceted answer for biological questions (Fig. 1A).

While imaging results are typically assessed visually to provide “yes or no” answers to determine if any differences exist, quantitative analyses of imaging experiments ultimately provide more objective insights into the data acquired. Image cytometry began with this initial purpose, to quantitatively describe cellular phenotypes together with spatial localization and morphology in two-dimensional images in an automated manner [3]. Such analytical methods have been successfully applied for simple nuclear stained cytospin preparations [4],

* Corresponding authors at: Singapore Immunology Network (SIgN), A*STAR (Agency for Science, Technology and Research), Biopolis, 8A Biomedical Grove, Singapore 138648, Singapore.
E-mail addresses: Ng_Lai_Guan@immunol.a-star.edu.sg (L.G. Ng), tan_yingrou@immunol.a-star.edu.sg (Y. Tan).

https://doi.org/10.1016/j.cellimm.2019.103946
Received 7 May 2019; Received in revised form 18 June 2019; Accepted 18 June 2019
Available online 02 July 2019
0008-8749/

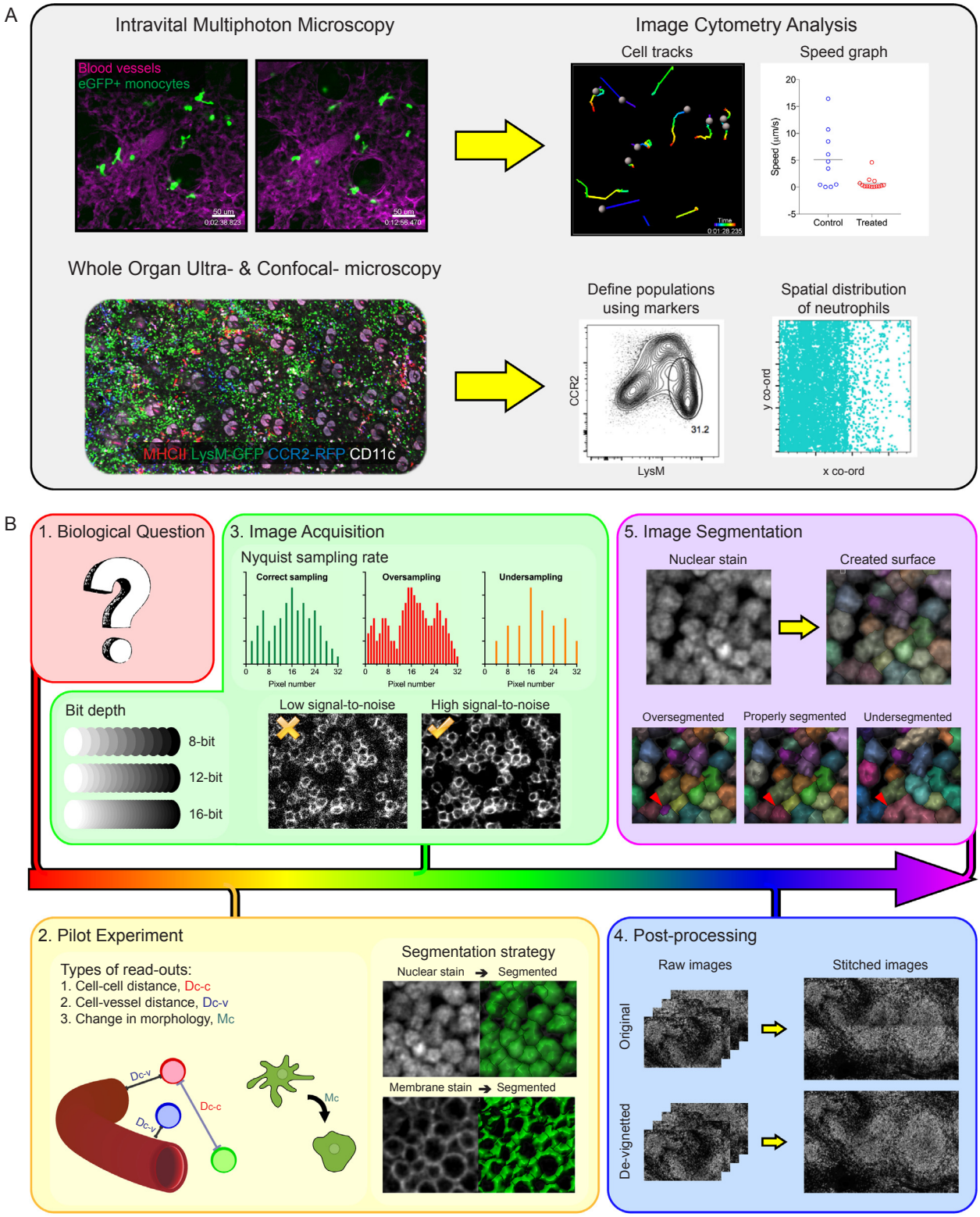

(caption on next page)

haematoxylin and eosin [5], immunohistochemically stained tissues and fluorescent *in situ* hybridization (FISH) preparations [6] for the last twenty years. Flow cytometry-style analysis of three-dimensional lymph node static image datasets, termed "histocytometry" [7], dynamic *in situ* cytometry (DISC) of intra-vital imaging datasets in spleen [8]; as well as correlated dynamic and static images obtained from the same tissue using "intra-vital dynamics-immunosignal correlative (iDISC) microscopy" [9] in recent years have further popularised this form of analysis in a tissue-based context. In this review, we highlight key technical aspects for which to pay attention, for the reader who may be

Fig. 1. Image Cytometry Workflow (A) Multi-modal Image Cytometry Approach. Intra-vital images of eGFP$^+$ monocytes in the lungs at two time-points using the multiphoton microscopy. Image cytometry analysis of intravital imaging allows for tracking of cellular behavior over space and time; relevant statistics obtained such as speed can be used for plotting graphs to compare cellular activity under different conditions. On the other hand, optical clearing can be coupled with whole organ imaging using the light sheet microscopy to obtain an overview of the spatial distribution of cells. Image cytometry allows for the spatial position of each cell to be mapped out in a 3-dimensional space. Where necessary, optically cleared samples can also be imaged using the confocal microscopy at higher magnification to achieve better resolution. (B) Tissue-based image cytometry workflow. (1) Biological question. A crucial step is to refine the biological question at hand and determine the type of information required to provide the answer. This will aid in deciding the appropriate imaging modality, image acquisition parameters, and image analysis strategy. (2) Pilot experiment. Trial runs minimise complexity of downstream analysis by providing biologists with a better idea of how and what to image, and the type of segmentation strategy to employ based on the desired read-outs. (3) Image acquisition. Acquisition parameters will affect the quality of images obtained and subsequently affect the quality of analysis. Biologists should consider the sampling rate, bit depth and factors that affect the signal-to-noise ratio in order to acquire images with the highest quality possible. (4) Post-processing. Post-processing steps such as de-vignetting, tile stitching, and deconvolution may be required before image segmentation is carried out on a whole complete image. (5) To achieve proper segmentation, biologists need to be meticulous in defining the boundaries between individual objects to derive accurate single-cell information. Over-segmentation or under-segmentation of images results in inaccurate representation of cellular features such as cell size, morphology, marker expression, and will affect the accuracy of downstream analysis.

interested to start image cytometry. We also discuss issues linked to sample preparation, image post-processing and analysis for intra-vital imaging and whole organ imaging.

2. Technical aspects of image cytometry

Prior to starting the experiment, it is crucial to consider the following question "Is imaging even the right tool to answer the biological question?" While imaging is a powerful tool to visually illustrate biological phenomenon, and great imaging data has the capability to blow audiences off their feet, it may not be worthwhile to do imaging solely for the "wow factor" it evokes. In many situations, alternatives such as flow cytometry could be more rapid and reliable for answering the question as imaging is time-consuming, requires specific technical expertise and the right infrastructure, and only allows for sampling of specific fields of view.

If imaging is the tool of choice, a typical tissue-based image cytometry workflow would involve the following steps: (1) image acquisition, (2) image post-processing (if necessary), (3) image segmentation, (4) flow cytometry-style quantitative analysis, (5) visualisation of cell subsets on image (if necessary). As this is a lengthy process where each step is linked and can take weeks from image acquisition to the end of analysis, it is important to bear in mind some important steps, and to answer some questions prior to imaging if image cytometry is the end-goal of imaging (Box 1). These include clarifying the biological question to be answered by imaging; determining whether the image obtained is suitable for image segmentation; acquiring quality raw data; carrying out image post-processing; identifying an appropriate image segmentation and analysis strategy and deciding on a software platform appropriate for analysis. Running pilot experiments is a critical step in identifying key technical issues early in the process (Fig. 1B).

Box 1. Questions for consideration during optimisation

General.

- What is the biological question to be answered using imaging?
- What sort of quantitative readouts are needed? (Eg. distance of cells to vasculature/ neurons)
- What sort of imaging modality and magnification is required?
- For the antibody panel, which antibody should be paired to which fluorophore?
- What type of image post-processing and segmentation steps is required? (Eg. are the stains membrane or cytoplasmic?)

For intra-vital imaging.

- What sort of drift compensation method is required?
- What sort of cell migration parameters and cellular changes need to be measured?

For optical clearing.

- Is it necessary to clear and image the entire organ? If not, what is the depth of the tissue that should be imaged?
- What is the general composition of the tissue to be cleared?
- Must the optical clearing method retain lipophilic dyes?
- What sort of computational pipeline is required for dealing with the large datasets?

Clarity about the biological question to be answered using imaging is critical to ensuring that the imaging sessions are productive. In considering the biological question, the experimental design should consider the type of quantitative readouts that could be provided by imaging. For instance, what is the distance of a certain cell type to vasculature or neurons or other cell subsets? Does the cell morphology, tortuosity of the vasculature or nerves change? Is the localization of cells within the tissue altered? Refining the scope of the question would aid in deciding the right imaging modality and resolution at which to acquire the images; it also provides a direction for image analysis later.

Next, pilot experiments should be run to determine the image segmentation strategy to be applied in downstream analysis, as image segmentation is typically a challenging process and is a crucial step to obtain accurate data for analysis [10]. In general, surface marker stains require different segmentation strategies in comparison to cytoplasmic and nuclear stains [11]; inhomogeneity in the distribution of the protein of interest within the cell can also lead to fluctuations in intensity within the image [12], making it harder to use certain segmentation approaches such as intensity thresholding. Running pilot experiments to understand whether the acquired images can be well-segmented, aids in choosing the right markers to minimise the complexity of downstream analysis. For instance, mast cells can be identified using either fluorophore-tagged avidin or anti-CD117 antibody. As CD117 antibody stains the cell membrane and avidin stains the cytoplasm, avidin would be a better choice for the staining panel to simplify downstream cell segmentation.

Next, the quality of the raw data acquired during imaging will affect the quality of the analysis. The dynamic range of the dataset depends on the bit depth of the images. The bit depth controls the range of grey-scale levels that are available in an image, and a 12-bit image would have 4096 shades of grey, while a 16-bit image has 65,536 levels. Charge-coupled devices (CCDs) or complementary metal oxide semiconductor (CMOS) cameras with which confocal or light sheet microscopes are equipped are typically 12-bit or 16-bit, while some microscope slide scanners have an option for recording 8-bit (red green blue) images or images with a higher bit depth. Images for image cytometry should have a higher bit depth to obtain a wider range for marker expression, particularly for cellular markers that are expressed at different levels. Acquired images should also be saved in a lossless file format such as the Tagged Image File Format to avoid any loss in information [13]. If quantitative analysis is the end-goal of imaging, it is also critical to ensure that there is no oversaturation in pixels during image

acquisition to avoid any loss of information, as any oversaturated pixel will have the same value.

Signal-to-noise ratio (SNR) is another important factor to keep in mind when deciding on the markers for imaging. A better SNR ratio makes it easier to differentiate if a pixel in the image belongs to the background or the foreground during image segmentation. Experiments involving fluorescent reporter proteins should take into account the relative brightness of reporter proteins [14] and the expression levels of the cells of interest. For example, *in vivo*, lysozyme M tagged with green fluorescent protein is approximately 5 times brighter in neutrophils as compared to macrophages. For immunolabelling experiments, a more specific antibody staining for immunostaining minimises the necessity for noise removal prior to image segmentation, particularly as it is easy for antibodies to be trapped in crevices within the tissue [15,16]. Careful planning of the fluorophore panel further ensures that markers with lower expression levels are imaged at spectra with less autofluorescence; line or frame averaging also aids in improving the SNR ratio [17]. Pilot experiments to optimise the appropriate imaging and immunolabelling conditions are indispensable for achieving quality raw data.

During image acquisition, care must also be taken to ensure that the sampling rate of the images is above the Nyquist sampling rate to ensure that there is sufficient spatial resolution in the image for reconstruction [18]. After acquisition of raw data, the images would be deconvolved to deblur the image using either deblurring or restoration algorithms. Deconvolution improves the signal to noise ratio of the image, and prepares it for quantitative image analysis [19]. However, it is important to note when imaging large volumes of tissues that it is typically not possible to image at resolutions required by the deconvolution program. In addition, deconvolution of large datasets is time consuming, and doubles the size of the data for storage (prior and after deconvolution).

Prior to image segmentation, image post-processing to deal with issues such as vignetting and tile stitching should be carried out if necessary. Vignetting occurs when there is uneven illumination of the acquired image, and this could affect the intensity of marker expression extracted for individual cells during analysis. Shading correction algorithms such as corrected intensity distributions using regularized energy minimization (CIDRE) [20], BaSIC [21] that are available on ImageJ or modules associated with CellProfiler [22] can be used to address this before tile stitching. Stitching algorithms [23,24] that are available on ImageJ as a plugin can then be used to put together individual image tiles.

Image segmentation is one of the critical steps in image cytometry to extract quality statistics for data analysis, and it cannot be emphasized enough that accurate segmentation is a non-trivial problem, particularly for three-dimensional datasets. Segmentation is used to: (1) separate the background from the objects of interest, (2) remove autofluorescent structures or antibody aggregates that may interfere with the image analysis process and (3) split closely touching objects. Background pixels can be separated from foreground pixels using thresholding, where an intensity "threshold" is selected such that pixels above the selected intensity are classified as actual signal. [13]. After background pixels are removed, each tissue and antibody panel should have a customised image segmentation strategy, as there may be different autofluorescent structures and differing membrane or cytoplasmic stains. Autofluorescent structures such as hair follicles or muscle that are present within tissues like skin contribute to the noise in the extracted data, and they can be removed using machine-learning pixel classification and segmentation programs such as ilastik [25]. Image segmentation of the structures of interest within the image will then be required to define the boundaries between individual objects to create computer-generated surfaces for feature extraction, where cellular features such as marker expression, cell morphology and spatial localization are obtained for analysis. Accurate segmentation is crucial to ensuring that cellular features extracted from the image are representative of the actual cells and distinguishing one cell from another becomes increasingly challenging in situations where there are large number of overlapping cells, for instance when immune cells infiltrate during inflammation. The difficulty in carrying out accurate segmentation of different cell types also varies, depending on the cell morphology. Round cells like leukocytes are easily dealt with, while cells with a dendritic-like morphology such as dermal epidermal T cells, macrophages and dendritic cells are significantly more difficult to segment properly. In dealing with difficult segmentation problems, a segmentation pipeline using a combination of different approaches such as feature detection, morphological filtering or region accumulation may be required. For further information, we would like to refer the reader to a review by Erik Meijering which provides a good overview of the different segmentation approaches [11].

Next, software platforms that integrate three-dimensional image segmentation algorithms with visualization capabilities such as the open-source FARSIGHT [26], Vaa3D [27,28], Microscopy Image Browser [29], CellProfiler 3.0 [30] and commercial image analysis programmes like Imaris, Volocity and Amira play an important role in image segmentation. In particular, programs that use surface-object rendering for visualizing segmented volumetric images allow users to interact with the surfaces to check for segmentation accuracy and to tweak segmentation parameters. As surface-object rendering is a time-consuming procedure, it is also important to check if important image metadata such as voxel size is accurately input into the program prior to starting analysis. In addition, the process of creating surfaces for multi-channel images can be streamlined so that the process of surface creation is simplified, and cell subsets are only defined later during analysis [31].

For analysis, software platforms that have an integrated analytical platform that allows the user to display cellular features in histogram, scatter plots or density plots streamline the process of data analysis. Ideally, the software should allow the user to interact with the data to further investigate different cell subsets through a flow-cytometry style process termed "gating". Alternatively, cellular features extracted out as a "comma separated values" (.csv) file can be automatically converted into "flow cytometry standard" (.fcs) files using the commercial software FlowJo for flow-cytometry style analysis. Specific cell subsets that have been gated out can then be re-visualised on the surface-objects rendered from the original image [31]. Ultimately, each software platform has different features, and time is needed for the user to become familiarised with each software interface. Thus, the user should decide which platform is most suitable for their analysis needs prior to starting.

To help familiarise the biologist with the terminologies and processes generally used in image analysis, we have compiled a list of useful articles (Box 2).

Box 2. Resources for image analysis

Topic	Reference
Image analysis glossary	[115]
Image analysis – basics and future perspectives	[13,116]
3-dimensional image visualisation and analysis	[117]
Beginner's guide for image acquisition	[18]
Overview of bioimage informatics	[10]
Overview of image segmentation approaches	[11]
Overview of analysis methods for cell profiling	[118]
Image deconvolution	[19]

3. Image cytometry for dynamic imaging

Intra-vital imaging provides the scientist with the capability to track

cellular behaviour, cell–cell interaction, cell proliferation or cell death within a living mouse over time and space. The generation of reporter mice where specific populations of cell types are labelled with fluorescent proteins was an important step forward for intra-vital imaging, as it made it possible to make observations with minimal perturbation of the biological system [32]. Mice expressing photoconvertible fluorescent proteins such as the Kikume Green-Red [33], the Kaede [34] and Dendra2 [35] are particularly useful for marking and tracking cell migration from a region of interest in tissues ranging from skin [36], orthothopic tumours [37] to germinal centers [38] in lymph nodes [39].

Prior to starting the imaging experiment, it is equally worthwhile to question how intra-vital imaging would value-add to answering the question, especially since intra-vital imaging requires technical expertise and specific reporter mice. Experimental design should include consideration of the tools required for achieving precision in the experimental readouts. While reporter mice have been traditionally used in intravital imaging experiments for tracking cellular movement, the next generation of reporter mice utilising optogenetic approaches to control cell migration may provide the researcher with increased control in experiments [40]. For instance, it is possible to trigger and stop cell migration with light using transgenic mice expressing photoactivatable chemokine receptor [41]. Next, the type of controls required when answering the biological question should also be within the same imaging experiment, and preferably within the same imaging field. For example, if the experiment is focused on investigating the migratory properties of neutrophils at different developmental stages, both neutrophil subsets, consisting of the proliferative neutrophil precursor and mature neutrophils, should be imaged simultaneously [42].

Prior to quantitative analysis of intra-vital images, a major issue that users must deal with is to minimise any image drift. Image drift can be particularly challenging for organs such as the lung [43] and heart [44,45], where there is inherently more motion within the tissue due to respiration or the heart beating. In severe cases, image drift can result in the loss of raw data when the region of interest moves out of the imaging window over time. Drift can be minimised using several strategies – mechanical stabilization of the tissue during imaging, active motion compensation using a tracking device; timed acquisition, as well as post-imaging processing [46–48]. Tissue preparation is a crucial part of minimising motion artefacts, and good surgery skills together with the appropriate mechanical stabilisers are critical for obtaining good raw data. When carrying out tissue preparation, it is crucial to bear in mind the delicate balance between adequate tissue stabilization and maintenance of tissues in a physiological state, as mechanical stabilization often requires some form of tissue compression. Over-compression could lead to the oxygen supply to the tissues being cut off, affecting the extent of the inflammatory response. Furthermore, some types of protocols may also involve delicate surgical procedures, and improper handling during surgery may induce undesired inflammation prior to imaging. As some tissue preparation procedures may be complex, detailed technical protocols [44,49] and video publications of the process would aid in overcoming the existing technical bottlenecks [50,51]. Active motion compensation requires more complex equipment and possibly modification of the microscope to track motion of the tissue to synchronise movement of either the objective lens or animal to minimise drift [52]. Timed acquisition requires knowledge of the displacement of the tissue over time, and acquisition is timed during periods where the organ experiences minimal motion [53]. An alternative to timed acquisition is triggering, where image acquisition is only triggered during an interval when the organ is more stable, such as the diastole phase of the heartbeat [45]. Post-imaging processing uses image registration and image reconstruction algorithms to deal with the image drift [54,55].

Due consideration should also be given to the readouts, as well as the way dynamic imaging data is visualised in a publication. Quantitative analysis for intra-vital datasets typically focuses on aspects such as cell migration, cell–cell interaction and changes such as cell proliferation and cell death. Track plots are helpful for identifying the migration patterns of individual cells; other readouts for migration parameters range from cell velocity, cell mean displacement to cell turning angles; durations of cell–cell interactions and cellular changes such as cell proliferation can also be measured. Uptake of extracellular material such as immune complexes or changes in cellular phenotype can further be detected in differences in the hue of a cell using labelled reagents or reporter mice such as the Fucci mice or $Ccr2^{RFP/+}/Cx3cr1^{GFP/+}$ mice [56–58]. Image panels are visually impactful and are useful for demonstrating a point. But it is crucial to note that two-dimensional projections of an image volume would not adequately show intracellular structures (such as uptake of extracellular material) or co-localization of structures, as these structures could be merely overlapping each other. In this case, X/Y and Y/Z cross-sections would better illustrate the point.

Additional analytical tools have been developed recently for intra-vital imaging, making it possible to monitor dynamic changes in blood vessel diameter, leakage and red blood cell velocity [59]. However, most of the quantitative readouts for intra-vital imaging are typically analysed in a scatter plot or histogram format. In order to analyse multi-parametric data from intra-vital images in a flow cytometry format, Philipp Bousso's group introduced Dynamic In Situ Cytometry (DISC) [8,60]. The advantage of this approach is the ability to subset cells based on their marker expression or within a spatial volume for further interrogation. Using DISC, they studied T cell motility when interacting with antigen-presenting cells bearing peptide-major histocompatibility complexes with differing affinities.

Cell tracking is a method by which the behaviour of individual cells is followed over time. Manual tracking is often a tedious process, and automated tracking algorithms aid in reducing the time needed for image processing. These algorithms work by carrying out two processes: (1) cell segmentation to distinguish the cellular signal from the background, and (2) cell association to connect segmented cells across time to obtain cellular tracks [61]. A cell tracking challenge comparing a number of state-of-art tracking algorithms for different datasets concluded that while some methods performed better than others, no method was fully accurate [62]. Evidently, further work needs to be carried out to improve automated cell tracking, and establishment of imaging databases like the leukocyte tracking database which have manually annotated live imaging datasets, can act as ground truth for testing tracking algorithms [63]. In the meantime, manual tracking by a user blinded to the cell subsets of interest would be the gold standard for attaining reliable cell tracks.

For a more in-depth treatment of intravital imaging, we would like to refer the reader to the article on intravital imaging in this issue, as well as an excellent primer on the subject by Germain *et al.* [64], Pittet *et al.* [65] and McArdle *et al.*[66].

4. Image cytometry for whole mount imaging

Immunofluorescence imaging typically focuses on a limited region of interest, with a limited penetration depth. In order to obtain clear and sharp images with minimal signal loss, tissues are typically sectioned into thin 10 μm sections for imaging. However, this makes it difficult to obtain an accurate three-dimensional representation of anatomical structures such as nerves or blood vessels which exist as a three-dimensional network [67]. One strategy to resolve this issue since the 1970s was to utilise serial two-dimensional sections and to reconstruct them to provide a three-dimensional view of the tissue [68,69]. However, artefacts could be introduced during sectioning, and reconstructing the tissue in three-dimensions is a tedious process involving complex image analysis procedures [70].

In order to image whole tissues, the technical issues of light scattering and light absorption within the tissue need to be resolved. Tissues are made up of different types of biomaterials, such as lipids,

proteins and cytoplasm, all of which scatter light differently, causing tissues to appear generally opaque. Chromophores within the tissue such as haemoglobin and melanin also absorb incident light. The combination of scattering and absorption of light results in opaque tissues; and as the composition of each tissue differs, the amount of light absorbed and scattered by each tissue type is also different [71]. The aim of optical clearing thus is to minimise lateral scattering and light absorption such that light can pass through the sample, rendering the opaque sample transparent in the process.

The push to optically clear tissues in recent years came mainly from the neuroscience field, which sought to describe neural circuits in a three-dimensional manner. Different optical clearing strategies were used in a bid to tackle the lipid-rich brain, which can be broadly divided into different categories including solvent-based, simple immersion, hyperhydration and hydrogel embedding methods [72]. Choosing the right optical clearing method for imaging the tissue of interest is crucial in ensuring that the refractive index of the tissue is matched, improving the signal-to-noise ratio of the images acquired. The quality of the images degrades significantly when there is a refractive index mismatch. Optical clearing methods that involve delipidation are not compatible with lipophilic dyes, while others may require prior optimizing with the antibody panel.

Solvent-based methods such as benzyl alcohol/ benzyl benzoate (BABB) [73,74], the DISCO methods [75–78] and ethyl cinnamate (ECi) [79], achieve optical clearing through removing water, followed by a delipidation step and refractive index matching with the remaining tissue. Simple immersion methods achieve optical clearing through refractive index (RI) matching, and high RI solutions containing sugar alcohols such as sucrose [80], fructose [81,82], iohexol [83], *N*-methylacetamide and Histodenz [84] are used to match the refractive index of the tissue. Urea forms a key component of hyperhydration methods such as Sca*l*e and CUBIC to drive the influx of water into the tissue [85]. This, in combination with delipidation with high detergent concentrations, followed by refractive index matching, achieves clearing [86]. Importantly, a heme eluting agent, Quadrol was found to decolourise blood-rich organs [87,88]. Hydrogel embedding methods started with the landmark Clear Lipid-exchanged Acrylamide-hybridized Rigid Imaging/Immunostaining/In situ hybridization-compatible Tissue-hYdrogel (CLARITY) method described by the Deisseroth group [89,90]. The localization of finer cellular structures such as proteins and nucleic acids is preserved by hybridizing biomolecules to an acrylamide hydrogel mesh with paraformaldehyde. Delipidation is then achieved through electrophoretic tissue clearing (ETC) using a high concentration of detergent combined with electrophoresis or without electrophoresis [91,92], followed by refractive index matching.

A typical protocol for preparing an organ for whole mount imaging would encompass the following steps: perfusion, tissue fixation, permeabilisation and immunolabelling (if required), optical clearing and imaging. Autofluorescence can be a significant issue when imaging whole tissues, both due to the presence of endogenous fluorophores like aromatic amino acids, the reduced form of nicotinamide adenine dinucleotide phosphate (NADPH), structural proteins like collagen and elastin, as well as residual blood within the vessels [93]. Proper perfusion of the mouse prior to tissue harvest aids in reducing autofluorescence due to blood. Chemical treatment of the tissue with sodium borohydride or Sudan black also aids in reducing tissue autofluorescence and improves signal-to-noise ratio in the green channel or approximately within 500–550 nm [94]. Finally, finding the optimal clearing method for each tissue is an iterative process where each new protocol seeks to resolve particular drawbacks in the protocol it was based on, hence there are a number of clearing protocols that are variations of the protocols published initially. Richardson and coworkers have written an excellent review covering the physics of optical clearing [72], while Susaki *et al.* [95] and Tainaka *et al.* [96] have also written comprehensive reviews detailing the chemical principles behind different optical clearing strategies.

Prior to starting an optical clearing experiment, the user should decide how to scope their optical clearing problem to minimize the technical challenges downstream. While it is technically possible and visually impactful to render whole organs transparent, as demonstrated by a number of optical clearing protocols, it may not be entirely necessary for answering the question of interest. Some worthwhile questions for users to ponder include: What sort of readouts would be relevant to the biological question? Is it necessary to image the entire organ or is a thick section sufficient? Must the clearing method retain lipids? What sort of experimental timeline is reasonable for each experiment? Is the biological question best answered by imaging at lower resolution using the light sheet microscope or at higher resolution using the confocal microscope or a combination of both? The time required for each step, whether it is immunolabelling, clearing, imaging or analysing, increases exponentially with the size of the tissue for imaging, and the biological question should be used to select the right optical clearing protocol and imaging modality. In general, imaging at lower resolution using the light sheet microscope provides a good overview of ongoing biological processes such as cell infiltration and localization in relation to vessels and nerves; following which, imaging at higher resolution using the confocal microscope can provide more detailed readouts for cell morphology and finer structures like epidermal nerves.

Next, thinking through the whole organ imaging computational pipeline is important for downstream image analysis processes, as imaging whole tissues usually generates large datasets ranging from a few gigabytes to 20 or 30 gigabytes. A computational pipeline together with the necessary hardware – large memory storage together with a good graphics card – should be established to deal with such large datasets, to facilitate rapid data transfer after image acquisition, and for image analysis [87]. Stitching of large datasets can be cumbersome using existing stitching algorithms, and stitching algorithms adapted to deal with large datasets such as TeraStitcher [97] or BigStitcher [98] help to accomplish this with limited computational resources. Three-dimensional visualization can then be carried out using proprietary software such as Imaris, Arivis, Amira, or freeware such as Vaa3D [27] or BigDataViewer in ImageJ [99]. Such software should have volume rendering speeds of at least 5 frames per second, to permit the user to interact with the image by rotating or zooming [27].

Data compression or downsizing could be used to improve the ease of the downstream computational steps when dealing with large datasets. One strategy is to compress images in a lossless format such as the Keller Lab Block (KLB) which is superior to other compression formats such as JPEG 2000 and LZW compression TIFF because of its high compression ratio, a fast read/write speed and the ability to utilise more central processing unit (CPU) cores [100]. Alternatively, images could be downsized by reducing the resolution and selecting only a portion of the dataset for analysis [86,87]. The disadvantage of such an approach is the loss of some information in the subsequent analytical steps.

The generation of whole organ image datasets, as optical clearing becomes increasingly accessible, would serve as a rich resource for the biological community. This can be accomplished by using image registration to a reference dataset using autofluorescence or structural images – such as the Allen Brain Atlas [101] for the neuroscience field [86,87,102,103]. Such a strategy enables the biologist to integrate data from individual studies together to provide a clearer overview of ongoing biological processes within the organ. Moving forward, the development of annotated organ maps such as the bone marrow, spleen, thymus or lymph node would be of great interest to the immunologist.

Following image registration, three-dimensional automated image segmentation pipelines can then be applied, bearing in mind that different segmentation strategies should be applied depending on the type of image obtained with the markers of interest [84,104]. Segmentation in three-dimensions is a non-trivial problem as many of the existing segmentation algorithms have been developed for two-dimensional

images. Segmentation in three-dimensions is more complex and requires increasingly greater computational power with larger datasets. While software packages like Volocity, Imaris and ImageJ may have spot counting algorithms, customized algorithms may be needed for specific purposes such as detecting single cell nuclei in a brain [102]. Subsequently, three-dimensional computer-generated surfaces should be generated based on the segmented images. For a large dataset, part of the difficulty would be rendering all the surfaces with limited computational power. One solution is to render these surfaces in a multi-resolution format, enabling the surfaces to be rendered quickly, making it possible for the user to interact with large datasets rapidly [105].

5. Conclusion and future perspectives

Interrogating a piece of tissue using a multi-modal imaging workflow quantitatively allows the biologist to correlate both temporal and spatial information of differing resolutions to provide an objective picture of ongoing biological processes. Recent development of newer techniques for multiplex imaging such as the Opal Vectra system by Perkin Elmer, tissue-based cyclic immunofluorescence (*t*-CyCIF) [106], co-detection by indexing (CODEX) [107] and imaging mass cytometry [108] make it possible to acquire high-dimensional imaging data, which was previously limited to four colours due to spectral overlap. Emerging single-cell spatial transcriptomic technologies in the form of highly multiplexed fluorescence *in situ* hybridization [109,110] and *in situ* RNA sequencing [111–113] further provide an avenue for deep characterisation of different cell populations within tissues. Such emerging techniques, in conjunction with development of newer tools for analysing high-dimensional spatial data [107,114] will further push the boundaries of the type of spatial imaging data that can be obtained in the future.

Acknowledgements

The authors would like to thank Leonard De Li Tan and Keith Weng Kit Leong for providing some of the images for the figure, Dr. Jackson Li Liang Yao who was instrumental in helping to set-up the image cytometry workflow in the Lai Guan Ng lab, as well as members of the lab for providing feedback on the manuscript.

Funding

This work was supported by the National Medical Research Council grant (NMRC/CSA-INV/0023/2017). This article is supported by Singapore Immunology Network (A*STAR) core funding to L.G.N. N.H. is supported by the A*STAR Graduate Scholarship (Singapore).

References

[1] R.A. Botting, K.M. Bertram, H. Baharlou, K.J. Sandgren, J. Fletcher, J.W. Rhodes, H. Rana, T.M. Plasto, X.M. Wang, J.J.K. Lim, L. Barnouti, M.P. Kohout, T. Papadopoulos, S. Merten, N. Olbourne, A.L. Cunningham, M. Haniffa, A.N. Harman, Phenotypic and functional consequences of different isolation protocols on skin mononuclear phagocytes, J. Leukoc. Biol. 101 (2017) 1393–1403.
[2] H. Gest, The discovery of microorganisms by Robert Hooke and Antoni Van Leeuwenhoek, fellows of the Royal Society, Notes and records of the Royal Society of London 58 (2004) 187–201.
[3] R.C. Ecker, G.E. Steiner, Microscopy-based multicolor tissue cytometry at the single-cell level, Cytometry. Part A : the journal of the International Society for Analytical Cytology 59 (2004) 182–190.
[4] G. Mehes, T. Lorch, P.F. Ambros, Quantitative analysis of disseminated tumor cells in the bone marrow by automated fluorescence image analysis, Cytometry 42 (2000) 357–362.
[5] J. Smolle, A. Gerger, W. Weger, H. Kutzner, M. Tronnier, Tissue counter analysis of histologic sections of melanoma: influence of mask size and shape, feature selection, statistical methods and tissue preparation, Analytical cellular pathology : the journal of the European Society for Analytical Cellular Pathology 24 (2002) 59–67.
[6] L.A. Kamentsky, D.E. Burger, R.J. Gershman, L.D. Kamentsky, E. Luther, Slide-based laser scanning cytometry, Acta Cytol. 41 (1997) 123–143.
[7] M.Y. Gerner, W. Kastenmuller, I. Ifrim, J. Kabat, R.N. Germain, Histo-cytometry: a method for highly multiplex quantitative tissue imaging analysis applied to dendritic cell subset microanatomy in lymph nodes, Immunity 37 (2012) 364–376.
[8] H.D. Moreau, F. Lemaitre, E. Terriac, G. Azar, M. Piel, A.M. Lennon-Dumenil, P. Bousso, Dynamic in situ cytometry uncovers T cell receptor signaling during immunological synapses and kinapses in vivo, Immunity 37 (2012) 351–363.
[9] G. Chodaczek, V. Papanna, M.A. Zal, T. Zal, Body-barrier surveillance by epidermal gammadelta TCRs, Nat. Immunol. 13 (2012) 272–282.
[10] H. Peng, Bioimage informatics: a new area of engineering biology, Bioinformatics 24 (2008) 1827–1836.
[11] E. Meijering, Cell Segmentation: 50 Years Down the Road [Life Sciences], IEEE Signal Process Mag. 29 (2012) 140–145.
[12] S. Dimopoulos, C.E. Mayer, F. Rudolf, J. Stelling, Accurate cell segmentation in microscopy images using membrane patterns, Bioinformatics 30 (2014) 2644–2651.
[13] V. Ljosa, A.E. Carpenter, Introduction to the quantitative analysis of two-dimensional fluorescence microscopy images for cell-based screening, PLoS Comput. Biol. 5 (2009) e1000603.
[14] T.J. Lambert, FPbase: a community-editable fluorescent protein database, Nat. Methods (2019).
[15] A. Joyner, N. Wall, Immunohistochemistry of whole-mount mouse embryos, CSH protocols pdb (2008 (2008)) prot4820.
[16] J.J. White, S.L. Reeber, R. Hawkes, R.V. Sillitoe, Wholemount immunohistochemistry for revealing complex brain topography, J. visualized experiments : JoVE (2012) e4042.
[17] J. Jonkman, C.M. Brown, Any Way You Slice It-A Comparison of Confocal Microscopy Techniques, J. biomolecular techniques : JBT 26 (2015) 54–65.
[18] A.J. North, Seeing is believing? A beginners' guide to practical pitfalls in image acquisition, J. Cell Biol. 172 (2006) 9–18.
[19] J.R. Swedlow, Quantitative fluorescence microscopy and image deconvolution, Methods Cell Biol. 114 (2013) 407–426.
[20] K. Smith, Y. Li, F. Piccinini, G. Csucs, C. Balazs, A. Bevilacqua, P. Horvath, CIDRE: an illumination-correction method for optical microscopy, Nat. Methods 12 (2015) 404–406.
[21] T. Peng, K. Thorn, T. Schroeder, L. Wang, F.J. Theis, C. Marr, N. Navab, A BaSiC tool for background and shading correction of optical microscopy images, Nat. Commun. 8 (2017) 14836.
[22] S. Singh, M.A. Bray, T.R. Jones, A.E. Carpenter, Pipeline for illumination correction of images for high-throughput microscopy, J. Microsc. 256 (2014) 231–236.
[23] S. Preibisch, S. Saalfeld, P. Tomancak, Globally optimal stitching of tiled 3D microscopic image acquisitions, Bioinformatics 25 (2009) 1463–1465.
[24] J. Chalfoun, M. Majurski, T. Blattner, K. Bhadriraju, W. Keyrouz, P. Bajcsy, M. Brady, MIST: Accurate and Scalable Microscopy Image Stitching Tool with Stage Modeling and Error Minimization, Sci. Rep. 7 (2017) 4988.
[25] C. Sommer, C. Straehle, U. Köthe, F.A. Hamprecht, Ilastik: Interactive learning and segmentation toolkit, in, IEEE International Symposium on Biomedical Imaging: From Nano to Macro 2011 (2011) 230–233.
[26] C.S. Bjornsson, G. Lin, Y. Al-Kofahi, A. Narayanaswamy, K.L. Smith, W. Shain, B. Roysam, Associative image analysis: a method for automated quantification of 3D multi-parameter images of brain tissue, J. Neurosci. Methods 170 (2008) 165–178.
[27] H. Peng, Z. Ruan, F. Long, J.H. Simpson, E.W. Myers, V3D enables real-time 3D visualization and quantitative analysis of large-scale biological image data sets, Nat. Biotechnol. 28 (2010) 348–353.
[28] H. Peng, A. Bria, Z. Zhou, G. Iannello, F. Long, Extensible visualization and analysis for multidimensional images using Vaa3D, Nat. Protoc. 9 (2014) 193–208.
[29] I. Belevich, M. Joensuu, D. Kumar, H. Vihinen, E. Jokitalo, Microscopy Image Browser: A Platform for Segmentation and Analysis of Multidimensional Datasets, PLoS Biol. 14 (2016) e1002340.
[30] C. McQuin, A. Goodman, V. Chernyshev, L. Kamentsky, B.A. Cimini, K.W. Karhohs, M. Doan, L. Ding, S.M. Rafelski, D. Thirstrup, W. Wiegraebe, S. Singh, T. Becker, J.C. Caicedo, A.E. Carpenter, Cell Profiler 3.0: Next-generation image processing for biology, PLoS Biol. 16 (2018) e2005970.
[31] Y. Tan, J.L.Y. Li, C.C. Goh, B.T.K. Lee, I.W.H. Kwok, W.J. Ng, M. Evrard, M. Poidinger, H.L. Tey, L.G. Ng, Streamlining volumetric multi-channel image cytometry using hue-saturation-brightness-based surface creation, Commun. Biol. 1 (2018) 136.
[32] T. Abe, T. Fujimori, Reporter mouse lines for fluorescence imaging, Dev. Growth Differ. 55 (2013) 390–405.
[33] S.L. Griswold, K.C. Sajja, C.W. Jang, R.R. Behringer, Generation and characterization of iUBC-KikGR photoconvertible transgenic mice for live time-lapse imaging during development, Genesis 49 (2011) 591–598.
[34] M. Tomura, N. Yoshida, J. Tanaka, S. Karasawa, Y. Miwa, A. Miyawaki, O. Kanagawa, Monitoring cellular movement in vivo with photoconvertible fluorescence protein "Kaede" transgenic mice, PNAS 105 (2008) 10871–10876.
[35] D.M. Chudakov, S. Lukyanov, K.A. Lukyanov, Tracking intracellular protein movements using photoswitchable fluorescent proteins PS-CFP2 and Dendra2, Nat. Protoc. 2 (2007) 2024–2032.
[36] M. Tomura, K. Kabashima, Analysis of cell movement between skin and other anatomical sites in vivo using photoconvertible fluorescent protein "Kaede"-transgenic mice, Methods Mol. Biol. 961 (2013) 279–286.
[37] D. Kedrin, B. Gligorijevic, J. Wyckoff, V.V. Verkhusha, J. Condeelis, J.E. Segall, J. van Rheenen, Intravital imaging of metastatic behavior through a mammary imaging window, Nat. Methods 5 (2008) 1019–1021.
[38] G.D. Victora, T.A. Schwickert, D.R. Fooksman, A.O. Kamphorst, M. Meyer-Hermann, M.L. Dustin, M.C. Nussenzweig, Germinal center dynamics revealed by multiphoton microscopy with a photoactivatable fluorescent reporter, Cell 143

(2010) 592–605.
[39] H.R. Hampton, J. Bailey, M. Tomura, R. Brink, T. Chtanova, Microbe-dependent lymphatic migration of neutrophils modulates lymphocyte proliferation in lymph nodes, Nat. Commun. 6 (2015) 7139.
[40] P. Tan, L. He, G. Han, Y. Zhou, Optogenetic Immunomodulation: Shedding Light on Antitumor Immunity, Trends Biotechnol. 35 (2017) 215–226.
[41] Y. Xu, Y.M. Hyun, K. Lim, H. Lee, R.J. Cummings, S.A. Gerber, S. Bae, T.Y. Cho, E.M. Lord, M. Kim, Optogenetic control of chemokine receptor signal and T-cell migration, PNAS 111 (2014) 6371–6376.
[42] Immunity 48 (2) (2018) 364–379.e8, https://doi.org/10.1016/j.immuni.2018.02.002.
[43] M.R. Looney, E.E. Thornton, D. Sen, W.J. Lamm, R.W. Glenny, M.F. Krummel, Stabilized imaging of immune surveillance in the mouse lung, Nat. Methods 8 (2011) 91–96.
[44] C. Vinegoni, A.D. Aguirre, S. Lee, R. Weissleder, Imaging the beating heart in the mouse using intravital microscopy techniques, Nat. Protoc. 10 (2015) 1802–1819.
[45] S. McArdle, G. Chodaczek, N. Ray, K. Ley, Intravital live cell triggered imaging system reveals monocyte patrolling and macrophage migration in atherosclerotic arteries, J. Biomed. Opt. 20 (2015) 26005.
[46] C. Vinegoni, S. Lee, P.F. Feruglio, R. Weissleder, Advanced Motion Compensation Methods for Intravital Optical Microscopy, IEEE journal of selected topics in quantum electronics : a publication of the IEEE Lasers and Electro-optics Society 20 (2014).
[47] C. Vinegoni, S. Lee, A.D. Aguirre, R. Weissleder, New techniques for motion-artifact-free in vivo cardiac microscopy, Front. Physiol. 6 (2015) 147.
[48] M. Vladymyrov, J. Abe, F. Moalli, J.V. Stein, A. Ariga, Real-time tissue offset correction system for intravital multiphoton microscopy, J. Immunol. Methods 438 (2016) 35–41.
[49] J.L. Li, C.C. Goh, J.L. Keeble, J.S. Qin, B. Roediger, R. Jain, Y. Wang, W.K. Chew, W. Weninger, L.G. Ng, Intravital multiphoton imaging of immune responses in the mouse ear skin, Nat. Protoc. 7 (2012) 221–234.
[50] B. Gligorijevic, D. Kedrin, J.E. Segall, J. Condeelis, J. van Rheenen, Dendra2 photoswitching through the Mammary Imaging Window, J. visualized experiments : JoVE (2009).
[51] C.C. Goh, J.L. Li, D. Becker, W. Weninger, V. Angeli, L.G. Ng, Inducing Ischemia-reperfusion Injury in the Mouse Ear Skin for Intravital Multiphoton Imaging of Immune Responses, J. visualized experiments : JoVE (2016).
[52] S.G. Yuen, D.T. Kettler, P.M. Novotny, R.D. Plowes, R.D. Howe, Robotic Motion Compensation for Beating Heart Intracardiac Surgery, Int. J. Robotics Res. 28 (2009) 1355–1372.
[53] S. Lee, C. Vinegoni, P.F. Feruglio, R. Weissleder, Improved intravital microscopy via synchronization of respiration and holder stabilization, J. Biomed. Opt. 17 (2012) 96018–196011.
[54] S. Lee, C. Vinegoni, M. Sebas, R. Weissleder, Automated motion artifact removal for intravital microscopy, without a priori information, Sci. Rep. 4 (2014) 4507.
[55] D. Soulet, A. Pare, J. Coste, S. Lacroix, Automated filtering of intrinsic movement artifacts during two-photon intravital microscopy, PLoS ONE 8 (2013) e53942.
[56] C. Sumen, T.R. Mempel, I.B. Mazo, U.H. von Andrian, Intravital microscopy: visualizing immunity in context, Immunity 21 (2004) 315–329.
[57] J.B. Beltman, A.F. Maree, R.J. de Boer, Analysing immune cell migration, Nat. Rev. Immunol. 9 (2009) 789–798.
[58] N. Zielke, B.A. Edgar, FUCCI sensors: powerful new tools for analysis of cell proliferation, Wiley interdisciplinary reviews, Dev. Biol. 4 (2015) 469–487.
[59] N. Honkura, M. Richards, B. Lavina, M. Sainz-Jaspeado, C. Betsholtz, L. Claesson-Welsh, Intravital imaging-based analysis tools for vessel identification and assessment of concurrent dynamic vascular events, Nat. Commun. 9 (2018) 2746.
[60] P. Bousso, H.D. Moreau, Functional immunoimaging: the revolution continues, Nat. Rev. Immunol. 12 (2012) 858–864.
[61] E. Meijering, O. Dzyubachyk, I. Smal, W.A. van Cappellen, Tracking in cell and developmental biology, Semin. Cell Dev. Biol. 20 (2009) 894–902.
[62] V. Ulman, M. Maska, K.E.G. Magnusson, O. Ronneberger, C. Haubold, N. Harder, P. Matula, P. Matula, D. Svoboda, M. Radojevic, I. Smal, K. Rohr, J. Jalden, H.M. Blau, O. Dzyubachyk, B. Lelieveldt, P. Xiao, Y. Li, S.Y. Cho, A.C. Dufour, J.C. Olivo-Marin, C.C. Reyes-Aldasoro, J.A. Solis-Lemus, R. Bensch, T. Brox, J. Stegmaier, R. Mikut, S. Wolf, F.A. Hamprecht, T. Esteves, P. Quelhas, O. Demirel, L. Malmstrom, F. Jug, P. Tomancak, E. Meijering, A. Munoz-Barrutia, M. Kozubek, C. Ortiz-de-Solorzano, An objective comparison of cell-tracking algorithms, Nat. Methods 14 (2017) 1141–1152.
[63] D.U. Pizzagalli, Y. Farsakoglu, M. Palomino-Segura, E. Palladino, J. Sintes, F. Marangoni, T.R. Mempel, W.H. Koh, T.T. Murooka, F. Thelen, J.V. Stein, G. Pozzi, M. Thelen, R. Krause, S.F. Gonzalez, Leukocyte Tracking Database, a collection of immune cell tracks from intravital 2-photon microscopy videos, Sci. Data 5 (2018) 180129.
[64] R.N. Germain, M.J. Miller, M.L. Dustin, M.C. Nussenzweig, Dynamic imaging of the immune system: progress, pitfalls and promise, Nat. Rev. Immunol. 6 (2006) 497–507.
[65] M.J. Pittet, R. Weissleder, Intravital imaging, Cell 147 (2011) 983–991.
[66] S. McArdle, Z. Mikulski, K. Ley, Live cell imaging to understand monocyte, macrophage, and dendritic cell function in atherosclerosis, J. Exp. Med. 213 (2016) 1117–1131.
[67] Y. Tan, W.J. Ng, S.Z.X. Lee, B.T.K. Lee, L.A. Nattkemper, G. Yosipovitch, L.G. Ng, H.L. Tey, 3-Dimensional Optical Clearing and Imaging of Pruritic Atopic Dermatitis and Psoriasis Skin Reveals Downregulation of Epidermal Innervation, J. Invest. Dermatol. (2018).
[68] C. Levinthal, R.W. Ware, Three Dimensional Reconstruction from Serial Sections, Nature 236 (1972) 207–210.
[69] R.W. Ware, Three-dimensional reconstruction from serial sections, Int. Rev. Cytol. 40 (1975) 325–440.
[70] M. Irla, J. Guenot, G. Sealy, W. Reith, B.A. Imhof, A. Serge, Three-dimensional visualization of the mouse thymus organization in health and immunodeficiency, J. Immunol. 190 (2013) 586–596.
[71] S.L. Jacques, Optical properties of biological tissues: a review, Phys. Med. Biol. 58 (2013) R37–R61.
[72] D.S. Richardson, J.W. Lichtman, Clarifying Tissue Clearing, Cell 162 (2015) 246–257.
[73] H.U. Dodt, U. Leischner, A. Schierloh, N. Jahrling, C.P. Mauch, K. Deininger, J.M. Deussing, M. Eder, W. Zieglgansberger, K. Becker, Ultramicroscopy: three-dimensional visualization of neuronal networks in the whole mouse brain, Nat. Methods 4 (2007) 331–336.
[74] K. Becker, N. Jahrling, S. Saghafi, H.U. Dodt, Immunostaining, dehydration, and clearing of mouse embryos for ultramicroscopy, Cold Spring Harbor protocols 2013 (2013) 743–744.
[75] A. Erturk, C.P. Mauch, F. Hellal, F. Forstner, T. Keck, K. Becker, N. Jahrling, H. Steffens, M. Richter, M. Hubener, E. Kramer, F. Kirchhoff, H.U. Dodt, F. Bradke, Three-dimensional imaging of the unsectioned adult spinal cord to assess axon regeneration and glial responses after injury, Nat. Med. 18 (2011) 166–171.
[76] A. Erturk, K. Becker, N. Jahrling, C.P. Mauch, C.D. Hojer, J.G. Egen, F. Hellal, F. Bradke, M. Sheng, H.U. Dodt, Three-dimensional imaging of solvent-cleared organs using 3DISCO, Nat. Protoc. 7 (2012) 1983–1995.
[77] N. Renier, Z. Wu, D.J. Simon, J. Yang, P. Ariel, M. Tessier-Lavigne, iDISCO: a simple, rapid method to immunolabel large tissue samples for volume imaging, Cell 159 (2014) 896–910.
[78] C. Pan, R. Cai, F.P. Quacquarelli, A. Ghasemigharagoz, A. Lourbopoulos, P. Matryba, N. Plesnila, M. Dichgans, F. Hellal, A. Erturk, Shrinkage-mediated imaging of entire organs and organisms using uDISCO, Nat. Methods 13 (2016) 859–867.
[79] A. Klingberg, A. Hasenberg, I. Ludwig-Portugall, A. Medyukhina, L. Mann, A. Brenzel, D.R. Engel, M.T. Figge, C. Kurts, M. Gunzer, Fully Automated Evaluation of Total Glomerular Number and Capillary Tuft Size in Nephritic Kidneys Using Lightsheet Microscopy, J. Am. Soc. Nephrol. JASN 28 (2017) 452–459.
[80] P.S. Tsai, J.P. Kaufhold, P. Blinder, B. Friedman, P.J. Drew, H.J. Karten, P.D. Lyden, D. Kleinfeld, Correlations of neuronal and microvascular densities in murine cortex revealed by direct counting and colocalization of nuclei and vessels, The Journal of neuroscience : the official journal of the Society for Neuroscience 29 (2009) 14553–14570.
[81] M.T. Ke, S. Fujimoto, T. Imai, SeeDB: a simple and morphology-preserving optical clearing agent for neuronal circuit reconstruction, Nat. Neurosci. 16 (2013) 1154–1161.
[82] M.T. Ke, T. Imai, Optical clearing of fixed brain samples using SeeDB, Current protocols in neuroscience, 66 (2014) Unit 2 22.
[83] M.T. Ke, Y. Nakai, S. Fujimoto, R. Takayama, S. Yoshida, T.S. Kitajima, M. Sato, T. Imai, Super-Resolution Mapping of Neuronal Circuitry With an Index-Optimized Clearing Agent, Cell reports 14 (2016) 2718–2732.
[84] W. Li, R.N. Germain, M.Y. Gerner, Multiplex, quantitative cellular analysis in large tissue volumes with clearing-enhanced 3D microscopy (Ce3D), PNAS 114 (2017) E7321–E7330.
[85] H. Hama, H. Kurokawa, H. Kawano, R. Ando, T. Shimogori, H. Noda, K. Fukami, A. Sakaue-Sawano, A. Miyawaki, Scale: a chemical approach for fluorescence imaging and reconstruction of transparent mouse brain, Nat. Neurosci. 14 (2011) 1481–1488.
[86] E.A. Susaki, K. Tainaka, D. Perrin, F. Kishino, T. Tawara, T.M. Watanabe, C. Yokoyama, H. Onoe, M. Eguchi, S. Yamaguchi, T. Abe, H. Kiyonari, Y. Shimizu, A. Miyawaki, H. Yokota, H.R. Ueda, Whole-brain imaging with single-cell resolution using chemical cocktails and computational analysis, Cell 157 (2014) 726–739.
[87] E.A. Susaki, K. Tainaka, D. Perrin, H. Yukinaga, A. Kuno, H.R. Ueda, Advanced CUBIC protocols for whole-brain and whole-body clearing and imaging, Nat. Protoc. 10 (2015) 1709–1727.
[88] K. Tainaka, S.I. Kubota, T.Q. Suyama, E.A. Susaki, D. Perrin, M. Ukai-Tadenuma, H. Ukai, H.R. Ueda, Whole-body imaging with single-cell resolution by tissue decolorization, Cell 159 (2014) 911–924.
[89] K. Chung, J. Wallace, S.Y. Kim, S. Kalyanasundaram, A.S. Andalman, T.J. Davidson, J.J. Mirzabekov, K.A. Zalocusky, J. Mattis, A.K. Denisin, S. Pak, H. Bernstein, C. Ramakrishnan, L. Grosenick, V. Gradinaru, K. Deisseroth, Structural and molecular interrogation of intact biological systems, Nature 497 (2013) 332–337.
[90] R. Tomer, L. Ye, B. Hsueh, K. Deisseroth, Advanced CLARITY for rapid and high-resolution imaging of intact tissues, Nat. Protoc. 9 (2014) 1682–1697.
[91] B. Yang, J.B. Treweek, R.P. Kulkarni, B.E. Deverman, C.K. Chen, E. Lubeck, S. Shah, L. Cai, V. Gradinaru, Single-cell phenotyping within transparent intact tissue through whole-body clearing, Cell 158 (2014) 945–958.
[92] J.B. Treweek, K.Y. Chan, N.C. Flytzanis, B. Yang, B.E. Deverman, A. Greenbaum, A. Lignell, C. Xiao, L. Cai, M.S. Ladinsky, P.J. Bjorkman, C.C. Fowlkes, V. Gradinaru, Whole-body tissue stabilization and selective extractions via tissue-hydrogel hybrids for high-resolution intact circuit mapping and phenotyping, Nat. Protoc. 10 (2015) 1860–1896.
[93] M. Monici, Cell and tissue autofluorescence research and diagnostic applications, Biotechnol. Annual Rev. 11 (2005) 227–256.
[94] A.S. Davis, A. Richter, S. Becker, J.E. Moyer, A. Sandouk, J. Skinner, J.K. Taubenberger, Characterizing and Diminishing Autofluorescence in Formalin-fixed Paraffin-embedded Human Respiratory Tissue, The journal of histochemistry

and cytochemistry : official journal of the Histochemistry Society 62 (2014) 405–423.
[95] E.A. Susaki, H.R. Ueda, Whole-body and Whole-Organ Clearing and Imaging Techniques with Single-Cell Resolution: Toward Organism-Level Systems Biology in Mammals, Cell Chem. Biol. 23 (2016) 137–157.
[96] K. Tainaka, A. Kuno, S.I. Kubota, T. Murakami, H.R. Ueda, Chemical Principles in Tissue Clearing and Staining Protocols for Whole-Body Cell Profiling, Annu. Rev. Cell Dev. Biol. 32 (2016) 713–741.
[97] A. Bria, G. Iannello, TeraStitcher - a tool for fast automatic 3D-stitching of teravoxel-sized microscopy images, BMC Bioinf. 13 (2012) 316.
[98] D. Hörl, F. Rojas Rusak, F. Preusser, P. Tillberg, N. Randel, R.K. Chhetri, A. Cardona, P.J. Keller, H. Harz, H. Leonhardt, M. Treier, S. Preibisch, BigStitcher: Reconstructing high-resolution image datasets of cleared and expanded samples bioRxiv (2018) 343954.
[99] T. Pietzsch, S. Saalfeld, S. Preibisch, P. Tomancak, BigDataViewer: visualization and processing for large image data sets, Nat. Methods 12 (2015) 481–483.
[100] F. Amat, B. Hockendorf, Y. Wan, W.C. Lemon, K. McDole, P.J. Keller, Efficient processing and analysis of large-scale light-sheet microscopy data, Nat. Protoc. 10 (2015) 1679–1696.
[101] E.S. Lein, M.J. Hawrylycz, N. Ao, M. Ayres, A. Bensinger, A. Bernard, A.F. Boe, M.S. Boguski, K.S. Brockway, E.J. Byrnes, L. Chen, L. Chen, T.M. Chen, M.C. Chin, J. Chong, B.E. Crook, A. Czaplinska, C.N. Dang, S. Datta, N.R. Dee, A.L. Desaki, T. Desta, E. Diep, T.A. Dolbeare, M.J. Donelan, H.W. Dong, J.G. Dougherty, B.J. Duncan, A.J. Ebbert, G. Eichele, L.K. Estin, C. Faber, B.A. Facer, R. Fields, S.R. Fischer, T.P. Fliss, C. Frensley, S.N. Gates, K.J. Glattfelder, K.R. Halverson, M.R. Hart, J.G. Hohmann, M.P. Howell, D.P. Jeung, R.A. Johnson, P.T. Karr, R. Kawal, J.M. Kidney, R.H. Knapik, C.L. Kuan, J.H. Lake, A.R. Laramee, K.D. Larsen, C. Lau, T.A. Lemon, A.J. Liang, Y. Liu, L.T. Luong, J. Michaels, J.J. Morgan, R.J. Morgan, M.T. Mortrud, N.F. Mosqueda, L.L. Ng, R. Ng, G.J. Orta, C.C. Overly, T.H. Pak, S.E. Parry, S.D. Pathak, O.C. Pearson, R.B. Puchalski, Z.L. Riley, H.R. Rockett, S.A. Rowland, J.J. Royall, M.J. Ruiz, N.R. Sarno, K. Schaffnit, N.V. Shapovalova, T. Sivisay, C.R. Slaughterbeck, S.C. Smith, K.A. Smith, B.I. Smith, A.J. Sodt, N.N. Stewart, K.R. Stumpf, S.M. Sunkin, M. Sutram, A. Tam, C.D. Teemer, C. Thaller, C.L. Thompson, L.R. Varnam, A. Visel, R.M. Whitlock, P.E. Wohnoutka, C.K. Wolkey, V.Y. Wong, M. Wood, M.B. Yaylaoglu, R.C. Young, B.L. Youngstrom, X.F. Yuan, B. Zhang, T.A. Zwingman, A.R. Jones, Genome-wide atlas of gene expression in the adult mouse brain, Nature 445 (2007) 168–176.
[102] T.C. Murakami, T. Mano, S. Saikawa, S.A. Horiguchi, D. Shigeta, K. Baba, H. Sekiya, Y. Shimizu, K.F. Tanaka, H. Kiyonari, M. Iino, H. Mochizuki, K. Tainaka, H.R. Ueda, A three-dimensional single-cell-resolution whole-brain atlas using CUBIC-X expansion microscopy and tissue clearing, Nat. Neurosci. 21 (2018) 625–637.
[103] W. Menegas, J.F. Bergan, S.K. Ogawa, Y. Isogai, K. Umadevi Venkataraju, P. Osten, N. Uchida, M. Watabe-Uchida, Dopamine neurons projecting to the posterior striatum form an anatomically distinct subclass, eLife 4 (2015) e10032.
[104] J. Stegmaier, F. Amat, W.C. Lemon, K. McDole, Y. Wan, G. Teodoro, R. Mikut, P.J. Keller, Real-Time Three-Dimensional Cell Segmentation in Large-Scale Microscopy Data of Developing Embryos, Dev. Cell 36 (2016) 225–240.
[105] S. Laine, T. Karras, Efficient sparse voxel octrees, IEEE Trans. Visual Comput. Graphics 17 (2011) 1048–1059.
[106] J.R. Lin, B. Izar, S. Wang, C. Yapp, S. Mei, P.M. Shah, S. Santagata, P.K. Sorger, Highly multiplexed immunofluorescence imaging of human tissues and tumors using t-CyCIF and conventional optical microscopes, eLife (2018) 7.
[107] Y. Goltsev, N. Samusik, J. Kennedy-Darling, S. Bhate, M. Hale, G. Vazquez, S. Black, G.P. Nolan, Deep Profiling of Mouse Splenic Architecture with CODEX Multiplexed Imaging, Cell, 174 (2018) 968-981 e915.
[108] C. Giesen, H.A. Wang, D. Schapiro, N. Zivanovic, A. Jacobs, B. Hattendorf, P.J. Schuffler, D. Grolimund, J.M. Buhmann, S. Brandt, Z. Varga, P.J. Wild, D. Gunther, B. Bodenmiller, Highly multiplexed imaging of tumor tissues with subcellular resolution by mass cytometry, Nat. Methods 11 (2014) 417–422.
[109] K.H. Chen, A.N. Boettiger, J.R. Moffitt, S. Wang, X. Zhuang, RNA imaging. Spatially resolved, highly multiplexed RNA profiling in single cells, Science 348 (2015) aaa6090.
[110] C.L. Eng, M. Lawson, Q. Zhu, R. Dries, N. Koulena, Y. Takei, J. Yun, C. Cronin, C. Karp, G.C. Yuan, L. Cai, Transcriptome-scale super-resolved imaging in tissues by RNA seqFISH, Nature (2019).
[111] P.L. Stahl, F. Salmen, S. Vickovic, A. Lundmark, J.F. Navarro, J. Magnusson, S. Giacomello, M. Asp, J.O. Westholm, M. Huss, A. Mollbrink, S. Linnarsson, S. Codeluppi, A. Borg, F. Ponten, P.I. Costea, P. Sahlen, J. Mulder, O. Bergmann, J. Lundeberg, J. Frisen, Visualization and analysis of gene expression in tissue sections by spatial transcriptomics, Science 353 (2016) 78–82.
[112] X. Wang, W.E. Allen, M.A. Wright, E.L. Sylwestrak, N. Samusik, S. Vesuna, K. Evans, C. Liu, C. Ramakrishnan, J. Liu, G.P. Nolan, F.A. Bava, K. Deisseroth, Three-dimensional intact-tissue sequencing of single-cell transcriptional states, Science 361 (2018).
[113] S.G. Rodriques, R.R. Stickels, A. Goeva, C.A. Martin, E. Murray, C.R. Vanderburg, J. Welch, L.M. Chen, F. Chen, E.Z. Macosko, Slide-seq: A scalable technology for measuring genome-wide expression at high spatial resolution, Science 363 (2019) 1463–1467.
[114] D. Schapiro, H.W. Jackson, S. Raghuraman, J.R. Fischer, V.R.T. Zanotelli, D. Schulz, C. Giesen, R. Catena, Z. Varga, B. Bodenmiller, histoCAT: analysis of cell phenotypes and interactions in multiplex image cytometry data, Nat. Methods 14 (2017) 873–876.
[115] A.H. Roeder, A. Cunha, M.C. Burl, E.M. Meyerowitz, A computational image analysis glossary for biologists, Development 139 (2012) 3071–3080.
[116] E. Meijering, A.E. Carpenter, H. Peng, F.A. Hamprecht, J.C. Olivo-Marin, Imagining the future of bioimage analysis, Nat. Biotechnol. 34 (2016) 1250–1255.
[117] F. Long, J. Zhou, H. Peng, Visualization and analysis of 3D microscopic images, PLoS Comput. Biol. 8 (2012) e1002519.
[118] J.C. Caicedo, S. Cooper, F. Heigwer, S. Warchal, P. Qiu, C. Molnar, A.S. Vasilevich, J.D. Barry, H.S. Bansal, O. Kraus, M. Wawer, L. Paavolainen, M.D. Herrmann, M. Rohban, J. Hung, H. Hennig, J. Concannon, I. Smith, P.A. Clemons, S. Singh, P. Rees, P. Horvath, R.G. Linington, A.E. Carpenter, Data-analysis strategies for image-based cell profiling, Nat. Methods 14 (2017) 849–863.